# NUMERICAL SIMULATION AND PARAMETER OPTIMIZATION OF COMBINED CUTTING AND CRUSHING FORAGE CRUSHER

/

# 铡切揉碎组合式牧草粉碎机数值模拟与参数优化

**Tao CHEN[1)], Shu-juan YI*[1)]; Song WANG[1)], Wen-sheng SUN[1)]**
College of Engineering, Heilongjiang Bayi Agricultural University, Daqing/P. R. China
*Tel: +86-459-13836961877; E-mile: yishujuan_2005@126.com*;
*Corresponding author: Shu-juan Yi*
*DOI: https://doi.org/10.35633/inmateh-75-08*

***Keywords:*** *forage; kneading machine; discrete element method; numerical simulation; parameter optimization*

## ABSTRACT

*The lack of effective visualization research methods for the crushing process of grass kneading has restricted the development of grass kneading machine to a certain extent. In this paper, the hay kneading process was numerically simulated by using the discrete element method, the stem movement rule, the mechanical characteristics of the stem particle group and the power consumption of the kneading were analyzed, and the motion and breaking mechanism of the grass in the hay kneading machine were defined. The effects of motor output speed and feed rate on the spinning rate and power consumption were studied. The regression equation between test factors and evaluation indexes was established. With the goal of maximizing the silk rates and minimizing the power consumption, the motor output speed and feeding amount are optimized and solved. The optimal parameter combination is determined as follows: when the output speed of the motor is 282.88 r/min and the feeding amount is 1.86 kg/s, the knead verification test shows that the silk rates is 92.88% and the power consumption is 3.68 kJ. The research results provide a reference for realizing high efficiency and low power consumption of grass kneading and parameter optimization of kneading device.*

## 摘要

*针对牧草揉丝破碎过程缺乏有效可视化研究方法，在一定程度上制约了牧草揉丝机发展进程的问题。本文以铡切揉碎协同式牧草揉丝机为研究对象，采用离散元方法对牧草揉丝过程进行数值模拟，对牧草茎秆运动规律、茎秆颗粒群力学特性、揉丝功耗进行分析，明确了牧草在揉丝机内运动和破碎机理。进行了台架多因素性能试验，研究了电机输出转速和喂入量对丝化率和功耗的影响，构建了试验因素和评价指标之间的回归方程。以丝化率最大化和功耗最小化为目标，对电机输出转速和喂入量进行优化求解，确定最优参数组合为：电机输出转速为282.88r/min、喂入量为1.86kg/s时，揉丝验证试验表明，丝化率为92.88%、功耗为3.68kJ。研究结果为实现牧草高效、低功耗揉丝和揉丝装置的参数优化提供参考。*

## INTRODUCTION

The kneading machine is a machine for processing and crushing forage grass (*Wu et al., 2022; Wang et al., 2017; Fan et al., 2021*). After kneading, the forage grass is filamentous with exposed internal nutrients (*Kang et al., 2021;Tang, 2023*), which can not only improve palatability, but also increase the contact area with the gastric juices of livestock, shorten the time of rumination and chewing, reduce the energy required for chewing of livestock, and have a better taste, which is convenient for the feeding and digestion of ruminant livestock (*Li et al., 2023; Wang et al.,2017; Pei et al., 2023*).

The contact between agricultural machinery and various agricultural materials and its impact on the design of agricultural machinery are important contents and difficulties in the digital design of modern agricultural equipment (*Shi et al., 2022*). As a computer numerical simulation method based on the discontinuity hypothesis, discrete element method can be used to simulate and analyze the interaction between agricultural materials and mechanical equipment, shorten the research and development cycle, and provide a means for the digital design of modern agricultural equipment, which has been widely used in the field of agricultural engineering (*Zeng et al., 2021*).

[1] *Tao Chen, Ph.D.; Shu-juan Yi, Prof. Ph.D.; Song Wang, Ph.D.; Wen-sheng Sun, Ph.D.*

Aiming at the problem of the lack of effective numerical simulation methods for the kneading and crushing process of corn stem, *Zhang Fengwei et al. (2019)* established a corn stem simulation model based on the discrete element method, and checked the parameters of the corn stem bonding contact model through the combination of physical and virtual tests, and finally conducted the crushing simulation and test verification for the corn stem discrete element model. *Geng Duanyang et al. (2021)* established a silage corn straw bonding model based on discrete element method, and carried out a silk kneading simulation test using EDEM to explore the effects of the number of teeth, two-roll differential ratio, the number of gap spiral turns and the driving roll speed on the silk ratio of straw. The relative error between the simulation test and the bench test results was 3.03%. *Zhang Tao et al. (2018)* used EDEM software to simulate the influence of the rotor speed of the hammer straw crusher on the straw conveying performance and the impact force of the straw, as well as the movement process of straw particle groups in the kneading chamber under different rotor speeds, providing a basis for the rotor speed optimization of the crusher. At present, the numerical simulation of forage crushing is mainly focused on crop straw, and rarely involves the research of forage. Therefore, it is necessary to further expand the research methods of forage crushing, and realize the visualization of forage crushing process by using convenient and economical research methods, so as to facilitate parameter optimization and control.

In this paper, the cooperative forage kneading machine for cutting and kneading was taken as the research object (*Chen et al., 2024*). The flexible alfalfa stem was established through the Hertz-Mindlin with Bonding contact model in EDEM software, the working process of the kneading machine was numerically simulated, and the movement rule of alfalfa stem in the kneading machine was observed. The mechanical properties of stem particle groups and the power consumption of kneading were studied under different working parameters. The research results can provide a reference for expanding the research methods of grass crushing, and solve the problem that the traditional physical method is difficult to visualize the material movement in the kneading machine.

## MATERIALS AND METHODS

### Structure and working principle

Cutting and kneading cooperative grass kneading machine is mainly composed of feeding conveyor belt, conveyor chain plate, feeding mechanism, screening mechanism, kneading mechanism, cutting mechanism and other parts. The structure is shown in Fig.1.

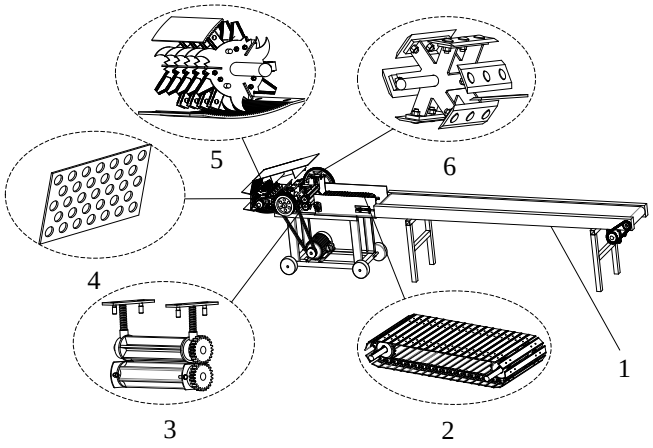


**Fig. 1 – Structural diagram of cutting and crushing cooperative forage kneader**

*1. Feeding conveyor belt; 2. Conveyor chain plate; 3. Feeding mechanism; 4. Screening mechanism; 5. Kneading mechanism; 6. Cutting mechanism*

The kneading operation is mainly divided into the following stages: feeding stage, the whole grass is transported to the conveyor chain plate through the feeding conveyor belt, and the grass enters the cutting chamber by rotation of the feed roller. In the cutting stage, the grass is cut into a certain length under the shearing action of the rotating motion of the grass knife and the fixed knife, and the cut grass is pushed to the kneading chamber under the rotation of the grass knife. In the kneading stage, the grass section is broken into filaments under the synergistic action of the hammer and serrated knife, the kneading and tearing between the hammer and serrated knife and the kneading tooth plate, the impact and friction between the sieve plate, etc.

In the screening and sending stage, the broken grass that meets the kneading length is thrown to the outside of the kneading machine through the screen plate under the combined action of the air flow generated by the rotation of the kneading rotor and the centrifugal force. The broken grass that is larger than the kneading length needs is kneaded in the kneading chamber for the next time, and further broken through the same crushing method as the last kneading until the length meets the kneading demand.

***Determination of alfalfa stem intrinsic parameters and establishment of discrete element model***

***Determination of intrinsic parameters***

The alfalfa used in the experiment was taken from the grass planting base in Duerbert County, Daqing City, Heilongjiang Province. The collected alfalfa was free from pests and diseases and there was no obvious mechanical damage. The average moisture content of alfalfa was determined by random sampling to be 78.4%. The stems were divided into root, middle and neck, and 100 mm stems were randomly intercepted as test materials. The diameter and length of the sample were measured using a digital display vernier caliper with an accuracy of 0.01 mm, and the distribution of stem samples and diameters was shown in Fig. 2.

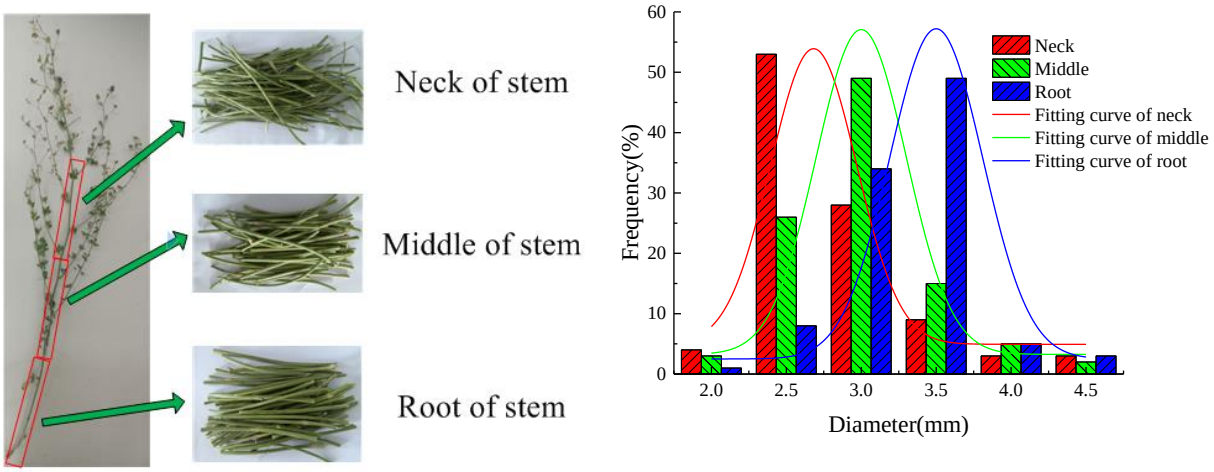


（a）Stem sample （b）Diameter distribution

**Fig. 2 - The sample and diameter distribution of alfalfa stem**

The average diameter and length of alfalfa stem root were 3.24 mm and 128.47 mm respectively. The average diameter in the middle is 3.13 mm and the length is 142.73 mm. The average diameter of the neck is 2.87 mm and the length is 151.12 mm.

**Contact model**

In this study, the discrete element simulation model of alfalfa stem adopts the Hertz-Mindlin with bonding contact model. In this model, two adjacent particles are connected by Bonding bond, and both ends of the bond are fixed on the connected spherical particles. The end of the bond can be deformed with the movement of the spherical particle, such as elongation, bending and torsion (*Wang et al., 2020; Zhang et al., 2023; Xie et al., 2023; Liu et al., 2022*). In the simulation, the fracture of bond was used to simulate the breaking process of alfalfa stem. The established alfalfa stem discrete element flexible model is shown in Fig. 3.

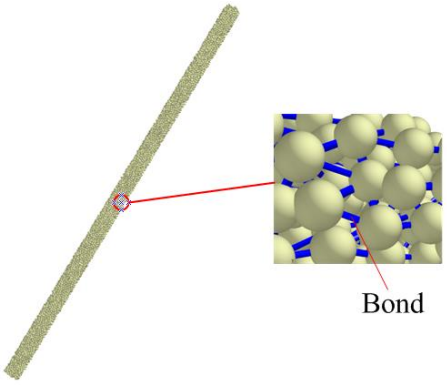


**Fig. 3 - Alfalfa stem discrete element flexible model**

**Simulation parameter**

According to the team's previous research results (*Chen et al., 2023*), the discrete element simulation parameters of alfalfa stem are shown in Table 1.

**Table 1**

**Simulation parameters of alfalfa stem**

| Parameter class | Name | Numerical value |
|---|---|---|
| Intrinsic parameters | Poisson ratio of alfalfa stem | 0.45 |
| | Poisson's ratio of steel plates | 0.30 |
| | Clover stem shear modulus / MPa | 17.5 |
| | Shear modulus of steel plate / Pa | $7.94\times10^{10}$ |
| | Alfalfa stem density /(kg·m$^{-3}$) | 996 |
| | Steel plate density / (kg·m$^{-3}$) | 7850 |
| Contact parameter | Alfalfa stem - alfalfa stem collision recovery coefficient | 0.44 |
| | Alfalfa stem - alfalfa stem static friction factor | 0.39 |
| | Alfalfa stem - alfalfa stem rolling friction factor | 0.13 |
| | Collision recovery coefficient of alfalfa stem and steel plate | 0.5 |
| | Static friction factor of alfalfa stem and steel plate | 0.5 |
| | Alfalfa stem and steel plate rolling friction factor | 0.2 |
| Bonding parameter | Normal contact stiffness / (N·m$^{-1}$) | $3.57\times10^{9}$ |
| | Tangential contact stiffness / (N·m$^{-1}$) | $4.01\times10^{8}$ |
| | Critical normal stress / Pa | $3.5\times10^{6}$ |
| | Critical tangential stress / Pa | $2.95\times10^{6}$ |
| | Bonding radius / mm | 0.5 |

***Numerical simulation of kneading and crushing process***

***Simulation model***

The 3D model of the kneading device was established in SolidWorks software. In order to improve the simulation efficiency, the simplified kneading device mainly includes feeding conveyor belt, conveying chain plate, feeding roller, cutting mechanism, kneading mechanism, screen plate, etc., which was saved as igs format and imported into EDEM 2020 software. The simulation model is shown in Fig. 4.

**Fig. 4 - Simulation model of guillotine cutting and crushing cooperative forage kneading machine**

**RESULTS AND DISCUSSIONS**

***Analysis of movement state of alfalfa stem***

The motion state of alfalfa stem during the kneading process in the simulation model was analyzed. At 0.3 s, the stems begin to be transported to the conveyor chain plate of the kneading machine, as shown in Fig. 5 (a). At 0.5 s, the stems begin to be transferred to the feed roller, as shown in Fig.5 (b). At 0.8 s, the stem begins to be transported to the cutting chamber, as shown in Fig. 5(c). At 1.4 s, the cut alfalfa segment begins to be pushed to the kneading chamber, as shown in Fig. 5 (d). At 2 s, stems that meet the kneading length are thrown out of the body through the sieve plate, as shown in Fig. 5(e). At 2.6 s, the stems are all fed into the kneading machine, as shown in Fig.5 (f).

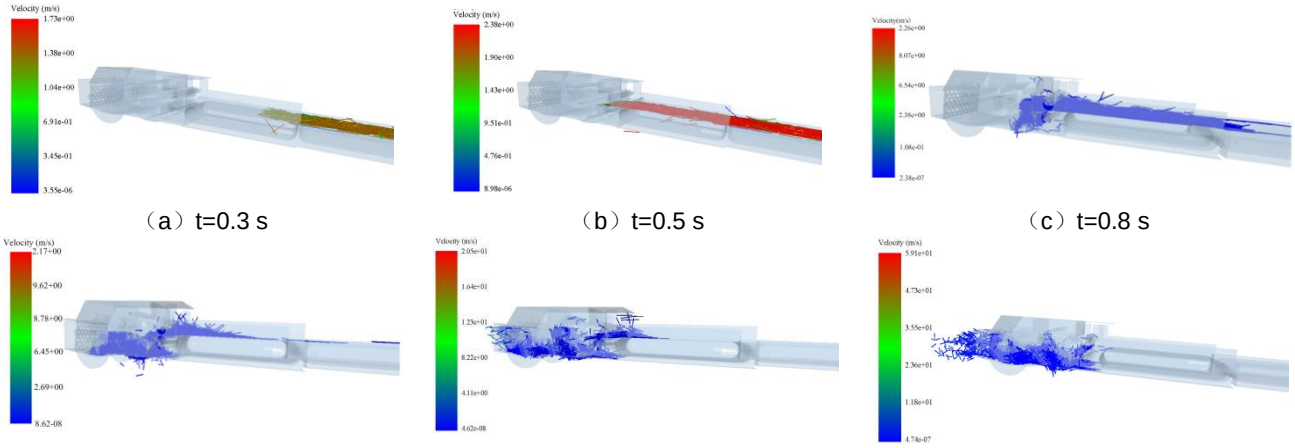

（a）t=0.3 s （b）t=0.5 s （c）t=0.8 s

（d）t=1.4 s （e）t=2 s （f）t=2.6 s

**Fig. 5 - Alfalfa stem movement at different time**

***Change analysis of bond quantity***

When the alfalfa stem model is broken, the bond between particles will be damaged and disconnected (*Liu et al., 2019; Leblicq T. et al., 2016; Liu et al., 2020*). At present, it is difficult to make quantitative statistics on the length of the material and the number of bonds contained after kneading. Therefore, this paper evaluated the effect of kneading machine crushing alfalfa stem by calculating the change of the number of all bonds in the domain.

In order to study the influence of rotor speed on the kneading effect, simulation was carried out under the motor output speed of 100 r/min, 200 r/min, 300 r/min, 400 r/min and 500 r/min respectively. According to the transmission ratio designed by the machine, the corresponding cutting shaft speed is 47 r/min, 94 r/min, 141 r/min, 188 r/min, 235 r/min; kneading shaft speed is 130 r/min, 260 r/min, 390 r/min, 520 r/min, 650 r/min; The effect of rotor speed on the number of bonds is shown in Fig. 6.

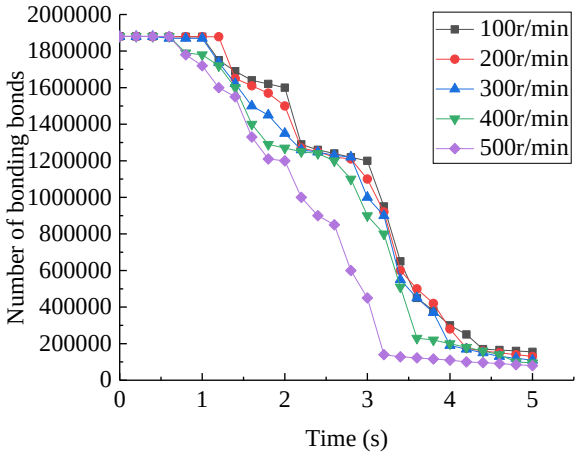


**Fig. 6 - The number of bonds varies under different motor output speed**

It can be seen from the Figure 6, that when t=0~0.5 s, the stem is in the transport process, and the number of bonds remains unchanged. When t=0.5~1.5 s, the stem is in the stage of cutting, and the bond gradually decreases at each speed, and the number of bonds decreases faster the higher the speed. From t=1.5~4 s, the number of bonds began to decrease sharply at each speed, indicating that the stem entered the kneading chamber and began to be kneaded. At this stage, the speed has a great influence on the change of the bond, and the obvious difference can be seen. The material in the kneading chamber is stable for 4~5 s, and the number of bonds basically remains unchanged. Through the analysis of the change of the number of bonds at different rotational speeds, it can be seen that with the increase of rotational speed, the kneading efficiency will also accelerate.

***Material quantity analysis in kneading machine***

In the EDEM software, three monitoring areas (Ⅰ, Ⅱ, Ⅲ) were established, as shown in Fig. 7, and the total number of alfalfa stems flowing through each interval was recorded, so as to calculate the change of the amount of materials at the cutting chamber, the kneading chamber and the discharge port with time at different rotating speeds.

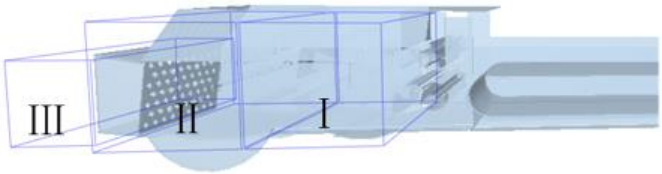


**Fig. 7 - Material quantity monitoring area**

***Guillotine cutting chamber***

The change of stem quantity in the cutting chamber under different rotation speed of the cutting shaft is shown in Fig. 8.

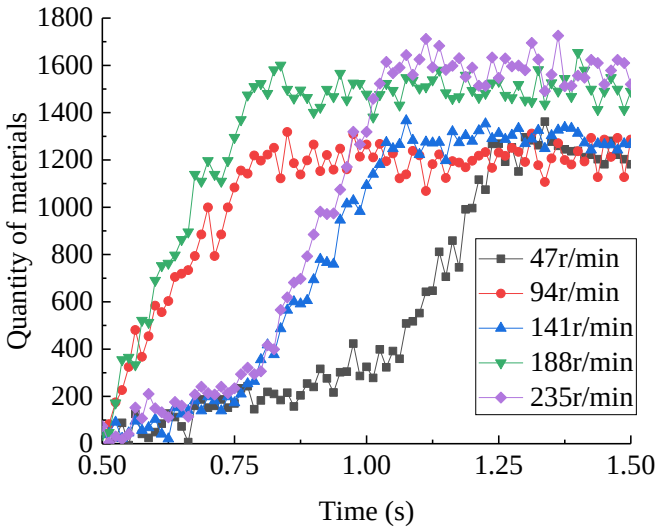


**Fig. 8 – The number of stem in the cutting chamber with time**

It can be seen from the figure that the number of stem in the cutting chamber under different cutting shaft speeds increases rapidly and shows a stable trend. After the number of stems was stabilized, the average number of stems in the knead chamber with the rotating speed of 47 r/min, 94 r/min, 141 r/min, 188 r/min and 235 r/min was 1085, 1170, 1224, 1532 and 1621, respectively, and then began to fluctuate around this number. The results showed that with the increase of the rotation speed of the cutting shaft, the number of stem cut in the cutting chamber in unit time also increased.

***Kneading chamber***

The changes in the amount of materials in the kneading chamber under different kneading shaft speeds are shown in Fig. 9.

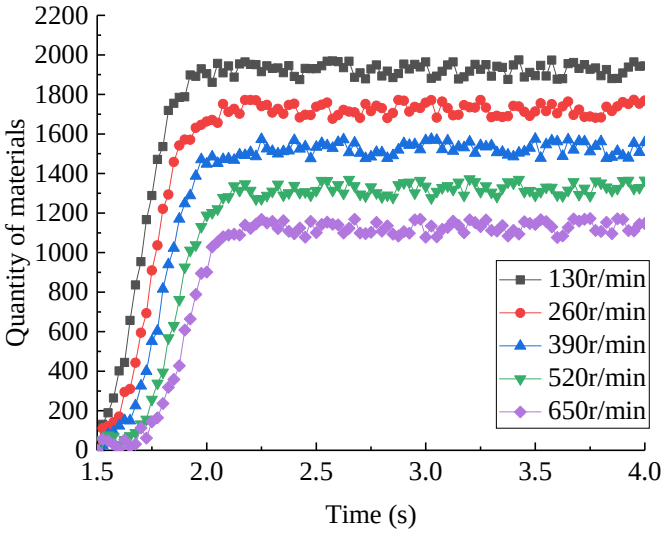


**Fig. 9 - The number of stems in the kneading chamber changes with time**

It can be seen from Fig. 9 that the number of stems in the kneading chamber increases rapidly and then shows a stable trend under different kneading shaft rotation speeds. After the number of stems was stabilized, the average number of stems in the knead chamber at 130 r/min, 260 r/min, 390 r/min, 520 r/min and 650 r/min were 1168, 1252, 1435, 1652 and 1836, respectively, and then began to fluctuate around this number. The results show that the amount of kneading machine per unit time increases with the increase of the rotational speed of the kneading shaft. The movement trajectory of the stem in the kneading chamber is shown in Fig.10.

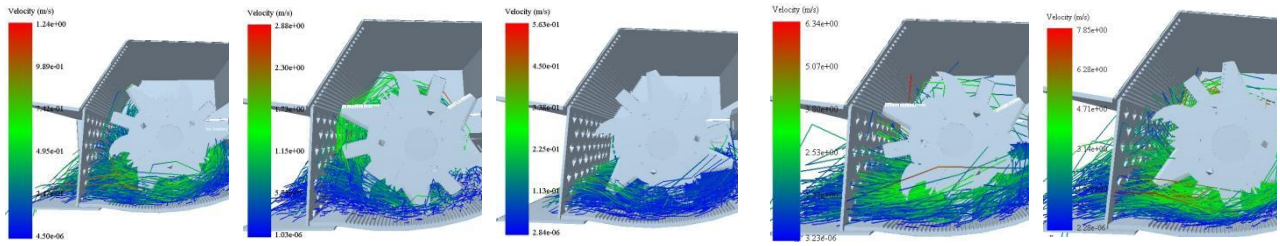

（a）r=130 r/min （b）r=260 r/min （c）r=390 r/min （d）r=520 r/min （e）r=650 r/min

**Fig. 10 - Stem movement trajectory in the kneading chamber**

***Discharge gate***

The change of the number of broken stems at the discharge port over time is shown in Fig. 11.

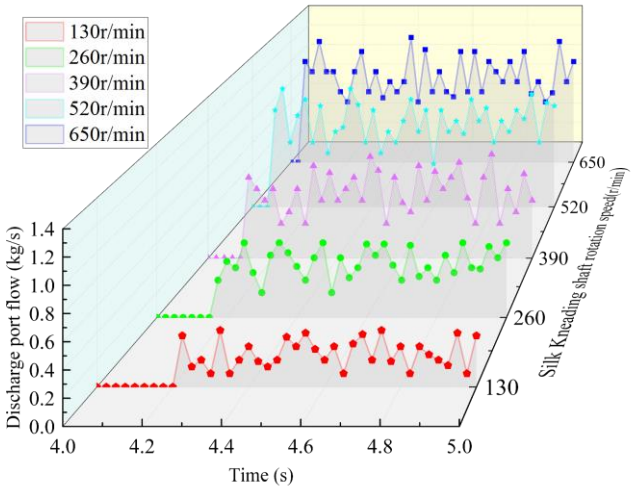


**Fig. 11 - Changes in the quantity of materials at the discharge port over time**

As can be seen from the figure, as the rotational speed of the kneading shaft increases, the number of broken stems at the discharge port also increases. When the rotational speed is lower than 260 r/min, due to the low interaction frequency between the stems and the kneading parts in unit time, the number of stems entering the kneading chamber in unit time is less, and the stems cannot be fully kneaded in a short time and cannot be timely screened, so the number of broken stems at the discharge port is less.

At 390 r/min, the stems can be broken in time, and there is almost no secondary kneading and circulation phenomenon. The silked stems can be stable and pass through the sieve, so the number of broken stems at the discharge port increases. When the rotational speed is higher than 520 r/min, due to the large centrifugal force on the stem, some of the longer stems that have not been fully kneaded are also directly discharged at the discharge port, so the amount of material at the discharge port increases significantly.

***Mechanical analysis of stem particle group***

Because there is only shear breakage for the alfalfa stem in the cutting chamber, the stress of the stem is relatively simple. However, in the kneading chamber, the stems are broken in various forms such as hitting, rubbing and impact, and the stress situation of the stems is more complicated (*Hu et al., 2020; Zhu et al., 2022*). Therefore, it is necessary to analyze the stress situation of the stem particle groups in the kneading chamber.

***Analysis of stem energy change***

The stem energy includes stem kinetic energy and potential energy. The influence of rotating speed of kneading axis on average stem energy is shown in Fig. 12.

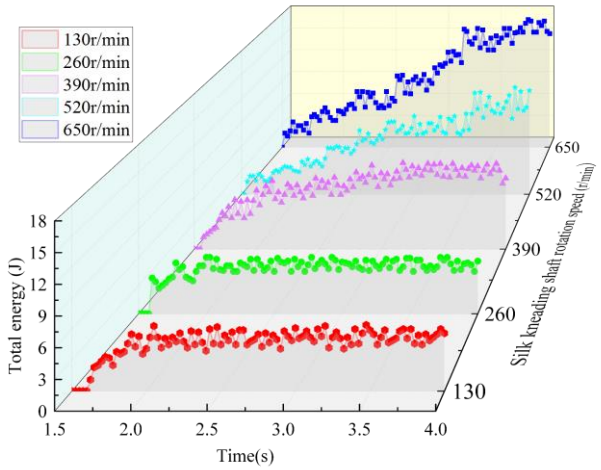


**Fig. 12 - Effect of rotating speed of kneading shaft on average energy of stem**

As can be seen from the figure, the average stem energy in the kneading chamber showed a trend of fluctuation and increase with the increase of the rotational speed of the kneading shaft. The average stem energy did not change significantly when the spindle speed increased from 130 r/min to 260 r/min. The average stem energy increased significantly when the spindle speed increased from 260 r/min to 650 r/min. The difference between the mean energy of stems at 390 r/min and that at 520 and 650 r/min increased with time.

**Mean stem to stem interaction force**

The influence of rotating speed of the kneading shaft on the average force between stems is shown in Fig.13.

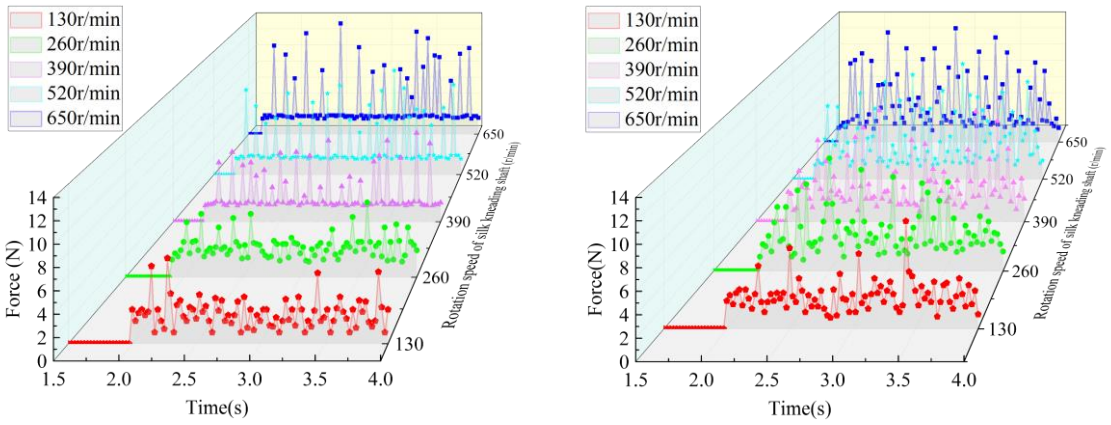


(a) Normal mean force (b) Tangential mean force

**Fig. 13 - Effect of rotating speed of kneading shaft on average stem to stem force**

As can be seen from the figure, the average stem to stem interaction force fluctuated sharply, and the fluctuation amplitude increased with the increase of the rotational speed of the kneading shaft. When the rotating speed of the kneading shaft was 130 r/min, 260 r/min, 390 r/min, 520 r/min and 650 r/min, the maximum normal forces of stem to stem could reach 7.2 N, 7.5 N, 9.3 N, 11.8 N and 13.5 N respectively. The maximum tangential mean force can reach 9.6 N, 10.9 N, 11.6 N, 12.9 N and 13.6 N respectively. The fluctuation of the average stem to stem interaction force is related to the random movement of a large number of stems in the kneading chamber, and the collision between the stems has a great influence on the movement of the stems in the kneading chamber. On the other hand, the increase of the rotational speed of the kneading shaft increases the energy of the stem, leading to the intensification of the collision between the stem, thus accelerating the energy loss of the stem itself, which is not conducive to the smooth screening of the stem.

**Mean stem to sieve plate interaction**

The influence of the rotating speed of the kneading shaft on the average force of the stem to sieve plate is shown in Fig.14.

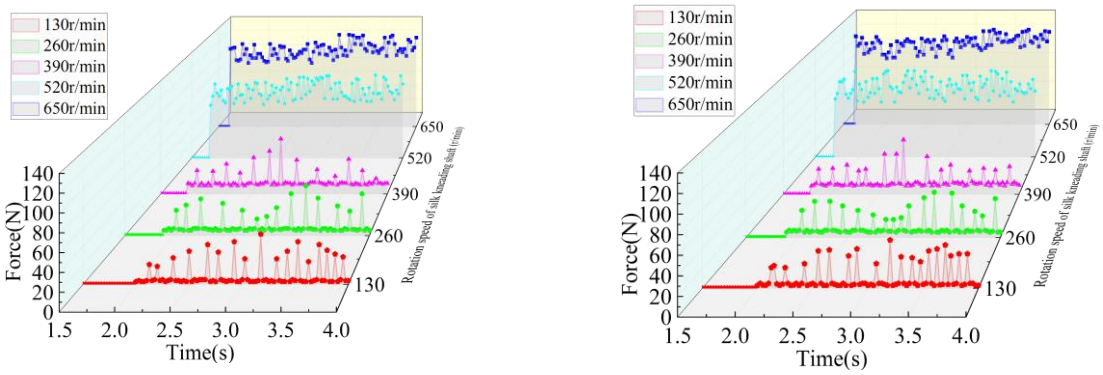


(a) Normal mean force (b) Tangential mean force

**Fig. 14 - Effect of the rotational speed of the wire kneading shaft on the average force between the crushing rod and sieve plate**

As can be seen from the figure, the average force of stem to sieve plate at different kneading shaft speeds all showed a fluctuating state after increasing from zero to a certain range. At 130 r/min, 260 r/min, 390 r/min, the mean interaction force of stem and sieve plate fluctuated sharply, and the maximum normal interaction force reached 53, 57, 68 N, and the maximum tangential interaction force reached 49, 50, 65 N, respectively. The fluctuation intensity of the average interaction force at 520 and 650 r/min is smaller than that at 130~390 r/min, and the maximum normal average interaction force can reach 110 and 130 N, and the maximum tangential average interaction force can reach 110 and 129 N, respectively. The increase of the rotational speed of the kneading shaft intensifies the collision between the stem and the sieve plate, resulting in a large amount of loss of the stem energy in the collision. Therefore, the rotational speed of the kneading shaft is not easy to be too fast under the premise of satisfying the quality of the kneading wire. The high-speed rotating hammer collides with the alfalfa section, thus providing the power for the alfalfa section to move. However, the collision between the alfalfa segment and the kneading chamber shell will consume the kinetic energy of the alfalfa segment. Therefore, in this paper, a serrated knife is installed on the kneading rotor of the cooperative grass kneading machine, which forms a staggered arrangement with the hammer in the axis to improve the distribution density of the kneading parts, so that it covers more kneading space in the work, and increases the frequency of interaction between the stem and the kneading parts per unit time. In order to increase the collision between the alfalfa segment and the kneading parts, and reduce the collision between the alfalfa segment and the kneading chamber shell, it is more beneficial to the movement of the alfalfa segment.

***Influence of different parameters on power consumption***

***Effect of rotational speed on power consumption***

The influence of rotation speed on power consumption is shown in Fig.15.

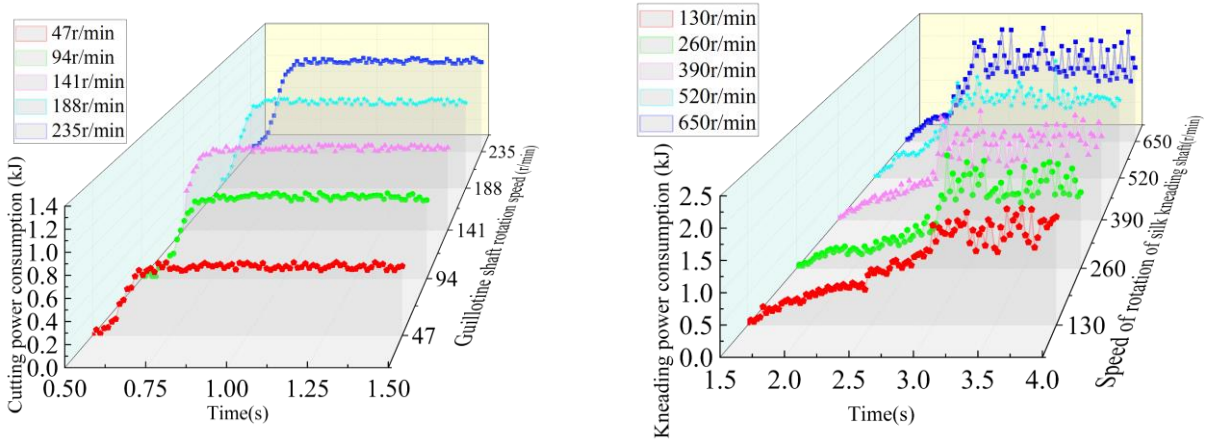


(a) Cutting shaft rotation speed (b) Rotation speed of the kneading shaft

**Fig. 15 - Influence of rotational speed on power consumption**

As can be seen from the figure, the fluctuation of the kneading power consumption is more severe than the cutting power consumption. Cutting power consumption and kneading power consumption are increased with the increase of rotor speed, the reason is that the speed increases, the number of interactions between the mechanical parts and the stem per unit time increases, and the power consumption increases. When the speed of the kneading shaft is lower than 260 r/min, the power consumption increases slowly, and when the speed reaches 390 r/min, the power consumption increases sharply, because the stem and the rotor rotate at the same speed, forming a material circulation layer, and the torque required for high speed is also greater. When the cutting shaft speed is 47, 94, 143, 188, 235 r/min, the average power consumption is 0.56, 0.71, 0.84, 0.94, 1.08k J, and the maximum is 0.66, 0.84, 0.91, 1.02, 1.14k J, respectively. When the rotating speed of the kneading shaft is 130, 260, 390, 520 and 650 r/min, the average power consumption of the kneading shaft is 1.39, 1.54, 1.76, 1.89 and 2.05 kJ, respectively, and the maximum power consumption is 1.89, 1.98, 2.06, 2.38 and 2.46 kJ, respectively.

***Influence of feeding amount on power consumption***

The influence of feeding amount on power consumption is shown in Fig. 16.

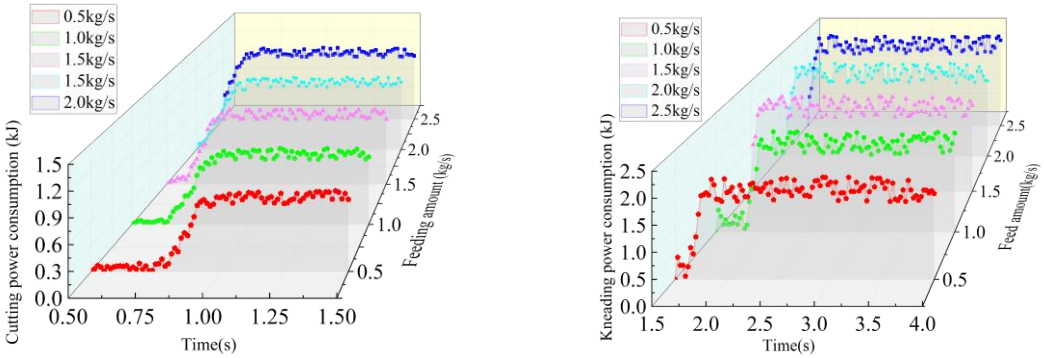


(a) Cutting power consumption (b) Kneading power consumption

**Fig. 16 - Influence of feeding amount on power consumption**

It can be seen from the figure that with the increase in the amount of feeding, the cutting power consumption and kneading power consumption are increased, the reason is that with the increase in the amount of feeding, the number of stems in the cutting chamber increases, the density of the stems in the cutting chamber and the kneading chamber increases, the impact force increases, the impact resistance of the cutting knife and the hammer increases, the friction between the stems leads to an increase in resistance, the number of collisions increases, resulting in an increase in power consumption. When the feeding amount is the same, the fluctuation of the kneading power consumption is more severe than that of the guillotine power consumption. When the feeding amount is 0.5, 1.0, 1.5, 2.0, 2.5 kg/s, the average power consumption of cutting is 0.57, 0.68, 0.81, 0.88, 0.99 kJ, and the maximum power consumption is 0.94, 0.97, 1.03, 1.06, 1.12 kJ, respectively. The average power consumption of kneading is 1.60, 1.61, 1.87, 1.98, 2.09 kJ, and the maximum power consumption is 1.97, 2.10, 2.13, 2.25, 2.32 kJ, respectively.

***Bench test***

The bench performance test was carried out on the self-developed kneading test bench, and the test was carried out in the crop harvest Laboratory of Heilongjiang Bayi Agricultural University, as shown in Fig. 17.


**Fig. 17 - Test site**

*1. Power consumption test device 2. Kneading machine 3. Feeding conveyor belt*

***Experimental design***

The evaluation indicators are calculated as follows:

*Silk rates*

Samples were collected at the outlet, at the same time interval for 3 times, each time no less than 200 g. All samples were mixed and weighed. Qualified alfalfa silk was screened and weighed, and its silk rate was calculated as:

$$W_h = \frac{m_1}{m_0} \times 100\% \quad (1)$$

where: $m_1$ is quality of alfalfa silk in the sample, g; $m_0$ is alfalfa sample quality, g.

*Power consumption*

The power consumption is determined by the DYN-200 torque power sensor installed on the motor spindle. After each group of tests, the instantaneous torque, power and required time measured by the sensor are derived through the torque measurement system, and the instantaneous power of the effective working period is calculated to obtain the kneading power consumption. The calculation formula is as follows:

$$W_z = \int P(t)dt_z \quad (2)$$

where: $W_z$ is kneading power consumption, kJ; $P(t)$ is instantaneous power, kW; $t_z$ is kneading time, s.

***Test results and analysis***

In the range of output speed 100~500 r/min and feed rate 0.5~2.5 kg/s, two-factor and five-level quadratic rotation orthogonal combination tests were carried out. The regression equation and optimization model between test factors and evaluation indexes are established by using Design-Expert 12.0 software. Factor coding is shown in Table 2. $x_1$ and $x_2$ are factor coding values, and the values in brackets in the table are rounded results according to actual operation requirements.

**Table 2**

**Test factor level table**

| Coding | Factor | |
|---|---|---|
| | Motor output speed $x_1$ (r/min) | Feeding quantity $x_2$ (kg/s) |
| 1.414 | 500 | 2.5 |
| 1 | 441.44（440） | 2.21（2.2） |
| 0 | 300 | 1.5 |
| -1 | 158.56（160） | 0.79（0.8） |
| -1.414 | 100 | 0.5 |

The test scheme and results are shown in Table 3.

**Table 3**

**Test scheme and results**

| Number | Motor output speed $x_1$ (r/min) | Feeding quantity $x_2$ (kg/s) | Silk rate $W_h$ (%) | Power consumption $Wz$ (kJ) |
|---|---|---|---|---|
| 1 | -1 | -1 | 90.49 | 3.31 |
| 2 | 1 | -1 | 90.31 | 2.99 |
| 3 | -1 | 1 | 97.27 | 4.26 |
| 4 | 1 | 1 | 91.97 | 3.88 |
| 5 | -1.414 | 0 | 91.36 | 3.92 |
| 6 | 1.414 | 0 | 90.96 | 3.16 |
| 7 | 0 | -1.414 | 89.67 | 3.37 |
| 8 | 0 | 1.414 | 96.37 | 4.21 |
| 9 | 0 | 0 | 92.26 | 3.38 |
| 10 | 0 | 0 | 92.18 | 3.35 |
| 11 | 0 | 0 | 91.07 | 3.36 |
| 12 | 0 | 0 | 91.28 | 3.26 |
| 13 | 0 | 0 | 91.41 | 3.48 |

The results of variance analysis of silk rate and power consumption are shown in Table 4 and Table 5 respectively.

**Table 4**

**Analysis of variance of silk rate**

| Source of variance | Sum of squares | Degree of freedom | Mean sum of squares | F | P |
|---|---|---|---|---|---|
| Model | 56.04 | 5 | 11.21 | 16.73 | 0.0009** |
| $x_1$ | 4.57 | 1 | 4.57 | 6.82 | 0.0348* |
| $x_2$ | 40.12 | 1 | 40.12 | 59.89 | 0.0001** |
| $x_1x_2$ | 6.55 | 1 | 6.55 | 9.78 | 0.0167* |
| $x_1^2$ | 0.13 | 1 | 0.13 | 0.19 | 0.6766 |
| $x_2^2$ | 4.4 | 1 | 4.4 | 6.56 | 0.0374* |
| Residual error | 4.69 | 7 | 0.67 | | |
| Lack of fit | 3.51 | 3 | 1.17 | 3.95 | 0.1089 |
| Error | 1.18 | 4 | 0.3 | | |
| Sum total | 60.73 | 12 | | | |

As can be seen from the table, the silk rate regression model ($P$=0.0009) is significant, while the loss of fit term ($P$=0.1089) is not, indicating that the model has a good degree of fitting and no loss of fit phenomenon occurs. The determination coefficient $R^2$=0.9228, the correction determination coefficient $R_{adj}$=0.8676, which is very close to 1, and the coefficient of variation is 0.89%, indicating that the test data is reliable. There is a significant relationship between the predicted value of the regression equation and the actual value obtained through the analysis of the test results. The regression equation of each factor and evaluation index obtained is shown as follows:

$$W_h = 91.64 - 0.76x_1 + 2.24x_2 - 1.28x_1x_2 - 0.14x_1^2 + 0.8x_2^2 \quad (3)$$

**Table 5**

**Analysis of power consumption variance**

| Source of variance | Sum of squares | Degree of freedom | Mean sum of squares | F | P |
|---|---|---|---|---|---|
| Model | 1.83 | 5 | 0.37 | 25.25 | 0.0002** |
| $x_1$ | 0.39 | 1 | 0.39 | 27.16 | 0.0012** |
| $x_2$ | 1.15 | 1 | 1.15 | 79.06 | < 0.0001** |
| $x_1x_2$ | 0.0009 | 1 | 0.0009 | 0.062 | 0.8104 |
| $x_1^2$ | 0.037 | 1 | 0.037 | 2.57 | 0.1526 |
| $x_2^2$ | 0.27 | 1 | 0.27 | 18.86 | 0.0034** |
| Residual error | 0.1 | 7 | 0.014 | | |
| Lack of fit | 0.077 | 3 | 0.026 | 4.14 | 0.1018 |
| Error | 0.025 | 4 | 0.006 | | |
| Sum total | 1.93 | 12 | | | |

As can be seen from the table, the power regression model ($P$=0.0002) is significant, while the loss of fit term ($P$=0.1018) is not, indicating that the model has a good degree of fitting and no loss of fit phenomenon occurs. The determination coefficient $R^2$=0.9475, the correction determination coefficient $R_{adj}$=0.9099, which is very close to 1, and the coefficient of variation is 2.99%, indicating that the test data is reliable. There is a significant relationship between the predicted value of the regression equation and the actual value obtained through the analysis of the test results. The regression equation of each factor and evaluation index obtained is shown as follows:

$$W_z = 3.87 - 0.22x_1 + 0.38x_2 - 0.02x_1x_2 - 0.07x_1^2 + 0.2x_2^2 \quad (4)$$

***Parameter optimization and test verification***

Design-Expert 12.0 software Optimization module was used to optimize the model with the goal of maximizing the silk rate and minimizing the power consumption, and the optimization mathematical model was established through the analysis.

$$\begin{cases} \max W_h(x_1, x_2) \\ \min W_z(x_1, x_2) \\ s.t. \begin{cases} -1.414 \le x_1 \le 1.414 \\ -1.414 \le x_2 \le 1.414 \end{cases} \end{cases} \quad (5)$$

The optimal parameter combination of the kneading machine is obtained as follows: when the output speed of the motor is 282.88 r/min and the feeding amount is 1.86 kg/s, the spinning rate is 93.13% and the power consumption is 3.63 kJ. At this time, the maximum value of the comprehensive evaluation index is 0.474, which is the optimal parameter combination, and the comprehensive evaluation response surface is shown in Fig. 18.

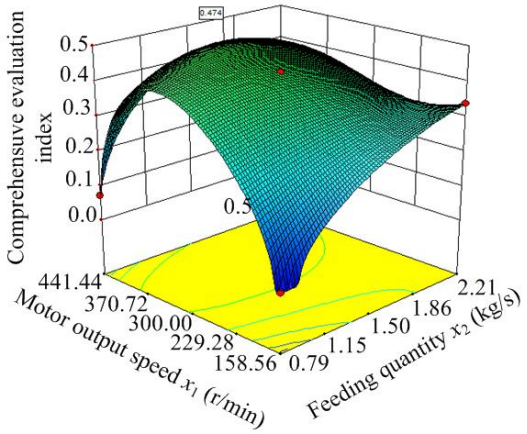


**Fig. 18 - Comprehensive evaluation response surface**

The bench verification test was carried out according to the optimal parameter combination obtained from the response surface analysis. In order to reduce the error, the test was repeated five times to take the average value, and the test results were as follows: the silk ratio was 92.88%, the power consumption was 3.68 kJ, and the difference between the actual test value and the software analysis value was 0.27% and 1.38%, respectively. The experimental results are close to the optimized values, which proves that the optimized results are accurate and reliable.

## CONCLUSIONS

(1) EDEM discrete element simulation software was used to simulate the working process of the kneading machine in different working parameters, and the law of stem movement, mechanical characteristics of stem particle groups and power consumption were analyzed, and the motion and crushing mechanism of the forage in the kneading machine were defined.

(2) The multi-factor test of bench performance was carried out, and the regression model of the spinning rate and power consumption was established. The variance analysis showed that the main and secondary factors affecting the spinning rate and power consumption were the feeding amount and the output speed of the motor.

(3) With the goal of maximizing the silk rate and minimizing the power consumption, the output speed and feeding amount of the motor were optimized by multi-objective solution, and the optimal parameter combination was obtained as follows: when the output speed of the motor was 282.88 r/min and the feeding amount was 1.86 kg/s. The verification test shows that the silk rate is 92.88% and the power consumption is 3.68 kJ, which meets the requirement of high moisture content alfalfa silk kneading.

## ACKNOWLEDGEMENT

This work was supported by National Natural Science Foundation of China (52275246) and Heilongjiang Bayi Agricultural University Graduate Innovative Research Project (YJSCX2023-Z02).

## REFERENCES

[1] Chunyong. T. (2019). Effects of different cutting lengths on Whole plant silage corn silage quality and beef cattle weight gain. *Sichuan Animal Husbandry and Veterinary Science*. Vol. 50, Issue 10 pp. 27-29.

[2] Decheng, W., Changbin, H., Hongjian, W., Yong, Y., & Guanghui, W. (2017). Review of Alfalfa Full-mechanized Production Technology. *Transactions of the Chinese Society for Agricultural Machinery*, Vol. 48, Issue 8, pp. 1-25.
[3] Defu, W., Mo, W., & Liqiao, L. (2017). Mechanism Analysis and Parameter Optimization of Hammer Mill for Corn stem. *Transactions of the Chinese Society for Agricultural Machinery*,) Vol. 48, Issue 11 pp. 165-171.
[4] Duanyang, G., Xiaodong, M., Yancheng, S., Yangmeng, Z., Huabiao, L., & Huixin, J. (2021). Simulation and Test of Silage Corn Screw Notched Sawtooth Type Crushing Roller. *Transactions of the Chinese Society for Agricultural Machinery*, Vol. 52, Issue 12 pp. 134-141.
[5] Fengwei, Z., Xuefeng, S., Xuekun, Z., Fangyuan, Z., Wancheng, W. & Fei, D. (2019). Simulation and experiment on mechanical characteristics of kneading and crushing process of corn straw. *Transactions of the CSAE*, Vol. 35, Issue 9, pp. 58-65.
[6] Gang, P., Zhiping, Z., Yuezheng, L., & Suchuan, S. (2023). Analysis of Coupling Motion Characteristics of Material and Airflow in Multi-function Forage Kneading Machine. *Transactions of the Chinese Society for Agricultural Machinery*, Vol. 54, Issue s2, pp. 156-163.
[7] Guoqiang, F., Zhongyu, W., Baoxing, W., Jinxing, W., Heyin, D., & Jian, H. (2021). Design and Experiment of Rotary Feed Tube Hammer Grinder. *Transactions of the Chinese Society for Agricultural Machinery*, Vol. 52, Issue 12 pp. 43-53.
[8] Haijun, Z., Yi, Q. & Haiqing, T. (2024). Design and Experimental Optimization of V-shaped Hammer for Hammer Mill. *INMATEH-Agricultural Engineering*, Vol. 73, Issue 2, pp.191-200.
[9] Hongcheng, L. (2023). *Study on Influence Mechanism and Optimization of the Hammer Mill Grinding Performance*. WuHan: Huazhong Agricultural University.
[10] Huibin, Z., Xian, W., Lizhen, B., Cheng, Q., Haoran, Z., & Hui, L. (2022). Development of the biaxial stubble breaking no-tillage device for rice stubble field based on EDEM-ADAMS simulation. *Transactions of the CSAE*, Vol. 38, Issue 19, pp. 10-22.
[11] Jianping, H., Jun, Z., Haoran, P., Wei, L., & Xingsheng, Z. Prediction (2020). Model of Double Axis Rotary Power Consumption Based on Discrete Element Method).*Transactions of the Chinese Society for Agricultural Machinery*, Vol. 51, Issue s1 pp. 9-16.
[12] Leblicq T., Smeets B., Vanmaercke S. (2016). A discrete element approach for modelling bendable crop stems. *Computers and Electronics in Agriculture*,124:141-149.
[13] Peng, L., Jin, H., Zhiqiang, Z., Caiyun, L., Zhenguo, Z., & Han, L. (2020). Kinematic Characteristic Analysis and Field Test of Chopped stem in Straw Retention Machine Based on CFD-DEM Coupling Simulation Method. *Transactions of the Chinese Society for Agricultural Machinery*, Vol. 51, Issue s1, pp. 244-253.
[14] Qirui, W., Hanping, M., & Qinglin, L. (2020). Simulation of Vibration Response of Flexible Crop Stem Based on Discrete Element Method. *Transactions of the Chinese Society for Agricultural Machinery*, Vol. 51, Issue 11 pp. 131-137.
[15] Ruijie, S., Fei, D., Wuyun, Z., Fengwei, Z., Linrong, S., & Junhai, G. (2022). Establishment of Discrete Element Flexible Model and Verification of Contact Parameters of Flax Stem. *Transactions of the Chinese Society for Agricultural Machinery*, Vol. 53, Issue 10, pp. 146-155.
[16] Tao, C., Shujuan, Y., Yifei, L., Guixiang, T., Shanmin, Q., & Rui, L. (2023). Establishment of Discrete Element Model and Parameter Calibration of Alfalfa Stem in Budding Stage. *Transactions of the Chinese Society for Agricultural Machinery*, Vol. 54, Issue 5 pp. 91-100.
[17] Tao, C., Shujuan, Y., Yifei, L., Guixiang, T., Xin, M., & Shanmin, Q. (2024). Design and Test of Cutting and Crushing Cooperative Silk Kneading Machine. *Transactions of the Chinese Society for Agricultural Machinery*, Vol. 55, Issue 5 pp. 149-159.
[18] Tao, Z., Fei, L., Manquan, Z., Qi, F., & Peng, Y. (2018). The Motion Law of Indoor Straw Swarm at Different Rotational Speeds Based on Discrete Element Method. *Agricultural Mechanization Research*, Vol. 40, Issue 9, pp. 195-19.
[19] Wei, X., Lei, P., Pin, J., Dexin, M., & Xiushan, W. (2023). Discrete Element Model Building and Optimization of Double-layer Bonding of Rape Shoots Stems at Harvest Stage. *Transactions of the Chinese Society for Agricultural Machinery*, Vol. 54, Issue 5, pp. 112-120.
[20] Weigang, L. (2019). Analysis of straw crushing characteristics and optimization of crushing equipment structure. Guiyang: Guizhou University.

[21] Xirui, Z., Xuhang, H., Junxiao, L., Youming, Y., & Yue, L. (2023). Calibration and Verification of Bonding Parameters of Banana Straw Simulation Model Based on Discrete Element Method. *Transactions of the Chinese Society for Agricultural Machinery*, Vol. 54, Issue 5, pp. 121-130.

[22] Yanbin, L., Yaoming L., & Tao Z. (2022). Effect of concentric and non-concentric threshing gaps on damage of rice straw during threshing for combine harvester. *Biosystems Engineering*, Vol. 219, pp.1-10.

[23] Yonggang, K., Yunqiong, L., & Guangqin, Z. (2021). Effects of kneaded Corn Straw microstorage on Growth Performance, Organ index and Blood Biochemical Indexes of Xuhuai Goats. *China Feed*, Vol. 17, pp.129-134.

[24] Zhiwei, Z., Xu, M., Xiulong, C., Zehua, L., & Xicheng, W. Critical (2021). Review of Applications of Discrete Element Method in Agricultural Engineering. *Transactions of the Chinese Society for Agricultural Machinery*, Vol. 52, Issue 4, pp. 1-20.